International Journal of Current Engineering and Technology
E-ISSN 2277 – 4106, P-ISSN 2347 - 5161

Available at http://inpressco.com/category/ijcet

Research Article

Optimizing 3D Sensor Network Topologies using Skeleton Extraction Algorithms

S. K. Pushpa[Ȧ*], S Ramachandran[Ḃ] and K. R. Kashwan[Ċ]

[Ȧ]S. K. Pushpa, Department of CSE, Vinayaka Missions University, Salem, India
[Ḃ]S. Ramachandran, Department of ECE, SJBIT, VTU, Bangalore, India
[Ċ]K. R. Kashwan, Department of ECE, Sona College of Technology, Anna University, Salem, India

Accepted 10 Sept 2014, Available online 01 Oct 2014, **Vol. 4**, **No. 5 Oct 2014)**

Abstract

Providing of additional resources to certain sensor nodes within the network has proved to improve network performance. To identify such nodes is a problem that exists in 3D topologies. To address this problem, skeleton extraction algorithm has been developed in an earlier work and the same is incorporated in this paper to optimize network performance in terms of network drop rate and sensor node energy. The skeleton extraction algorithm considers realistic complex 3D space models for sensor node coverage rendering it practical and applicable to the real world deployments. A novel energy utilization function is discussed to identify the skeletal links and skeleton nodes. The skeleton extracted is represented as a graph and the topological features of the 3D deployment spaces are preserved using clustering techniques. The experimental study presented considers complex 3D deployment scenarios. The simulation results prove that if additional resources are provided to the skeleton nodes identified, the network performance is enhanced and energy conservation achieved is about 20%.

Keywords: *Complex 3D space, protocol, wireless sensor networks, skeleton extraction algorithm, critical node, skeleton node*

1. Introduction

The application of Wireless sensor networks for monitoring habitats (R. Szewczyk *et al*, 2004), medical systems (Kumar. P *et al*, 2010), surveillance (M. Fennell *et al*, 1998), disaster relief etc. are well established (M. Younis *et al*, 2008). A wireless sensor network consists of sensor nodes which are identified by their constrained capabilities in processing, energy resources, sensing ranges and radio transmission ranges. Accurate data aggregation techniques coupled with energy efficiency and network overhead reduction are critical to achieve the perceived goals of sensor network deployments. A sensor node placement strategy which is a part of network design is critical to achieve complete coverage in terms of sensing and communication (Yonghyun Kim *et al*, 2012).

Topology generation is one of the major problems in WSN as sensor nodes get depleted at the earliest because of its battery constraints. Provisioning of additional energy resources to certain sensor nodes enhances the performance of sensor networks proved by the research presented in Ref. (Zhao Cheng *et al*, 2008). The identification of the critical sensor nodes in sensor networks is a problem that needs to be solved. To identify such critical nodes, a new skeleton extraction algorithm is designed for 3D sensor networks. Sensor coverage is a primary design factor considered for wireless sensor network deployments. 2D ideal plane (X. Bai *et al*, 2008, S. Kumar *et al*, 2005) or 3D full space models (C. F. Huang *et al*, 2004, M. Watfa *et al*, 2006) is considered but these models are inaccurate when applied to actual sensor network deployments. A recent study described presented by (Linghe Kong *et al*, 2013) proves that the coverage of sensor networks in practical environments is a 3D complex space and short comings of the existent sensor coverage models are clearly described. In Ref. (Linghe Kong *et al*, 2013), the authors cite the Tungurahua volcano monitoring project (http://fiji.eecs.harvard.edu/Volcano/.) and define the Coverage Dead Zone problem that exists by adopting 2D surface coverage model for 3D sensor networks or ideal sensor network deployments. In addition to the coverage dead zone, non-existent links are also established.

To clearly understand the error in the network connectivity, let us consider a sensor deployment of seven sensor nodes labelled Node A to Node G on an elevated terrain shown in Fig. 1. The dotted line represents the actual network connectivity that exists. The 2D projection of this topology is also shown in Fig. 2 and from this figure, it can be noticed that the link between Node B and Node E (described by a thick red line) exists, which is not true considering 3D complex deployments of wireless sensor networks as the nodes are not within the radio range. The coverage dead zone and the inaccuracies in the network and radio layer can be eliminated by considering 3D sensor network deployments as complex spaces. In this

*Corresponding author: **S. K. Pushpa**

paper, we have adopted the 3D deployments for complex spaces to achieve idealistic results applicable to the real world scenarios. A complex space is a terrain with lot of ups and downs.

In order to identify the critical nodes, a novel skeleton extraction mechanism is proposed in this paper. Skeleton Extraction techniques have been applied to varied fields like computer vision (N. D. Cornea *et al*, 2005), image processing (J. W. Brandt *et al*, 1992), computer graphics (N. Gagvani *et al*, 2001), and medical image processing (S. R. Aylward *et al*, 2002). The skeleton extraction techniques cannot be directly adopted to address the problem in sensor networks owing to the discrete nature exhibited by sensor network deployments. The discrete nature is exhibited by the skeleton extraction as the skeletons of sensor networks are dependent on the network connectivity and the topological position of sensor nodes and not the topological information alone.

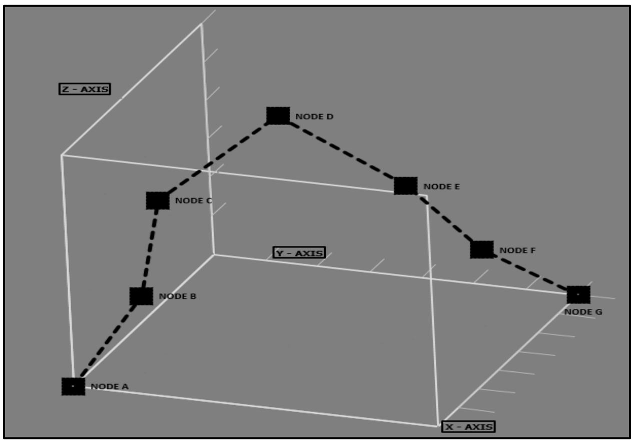

Fig.1 A Seven Sensor Node Topology in 3D Surface (S. K. Pushpa *et al*, 2013)

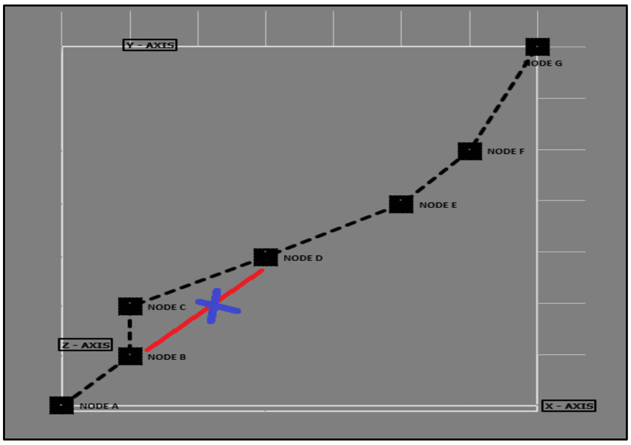

Fig.2 Network Layer/Radio Layer Error While Applying 2D Models to 3D Topologies of Sensor Networks (S. K. Pushpa *et al*, 2013)

The hop based approach is utilized in computing the distances and not the Euclidian distance method as adopted in generic skeleton extraction techniques. The hop based distance computation induce noise and the regular skeletal extraction suffers accuracy in the presence of noise (J. Bruck *et al*, 2005) and, therefore, even the 3D skeletal extraction algorithms cannot be directly adopted in the case of sensor networks. The skeleton extraction in wireless sensor networks reported in references (J. Bruck *et al*, 2005, Hongbo Jiang *et al*, 2010, Wenping Liu *et al*, 2013) consider only 2D deployments and not 3D complex deployments, which is a major motivating factor of the research work using 3D skeleton extraction presented here.

In this paper, a skeleton extraction technique is proposed for 3D complex deployments of sensor networks. The skeleton is represented as a graph consisting of skeletal links and skeleton nodes. To identify the skeletal links, transmissions are carried out throughout the network from a node to all the other sensor nodes recursively. The energy utilized is monitored and the skeletal links are identified by the energy utilization function, a feature that is introduced in this paper. Backtracking the skeletal links provide the skeleton nodes and enable redundant link elimination. The root node of the skeleton graph is the sensor node and is a part of all the skeletal links and is identified on the basis of the frequency based weight assignment function. To eliminate the loss of topological information in the skeleton graph, the sensor network is topologically clustered to construct the layered topological sets and the position of the skeleton nodes is derived on the basis of a novel distance function.

This paper is organized as follows. Section two describes literature survey of the work carried out by researchers in the area of skeleton extraction. The proposed Skeleton Extraction technique is presented in the third section. The Implementation of the Skeleton Extraction Algorithm is presented in the penultimate section and the conclusions are drawn in the last section.

2. Literature survey

Skeletal extraction is applied to varied fields like image processing, biomedical applications, and computer vision and graphics. A comprehensive study of the varied skeleton extraction techniques, its applications and properties are described in Ref. (Cornea N. D *et al*, 2007) and the techniques are classified into four categories mentioned below.

a. Thinning and boundary based Skeleton Extraction for digital topologies: A thin line is used to represent the skeleton and is achieved by the repeated shrinking of objects defining a digital topology. The thinning and boundary based techniques present huge computational times to converge and hence researchers have also proposed parallelization techniques to reduce the computational time (D.G. Morgenthaler *et al*, 1981).
b. Distance Field Based Skeleton Extraction for digital topologies: Generally a three step approach is adopted in this technique. The first step is a ridge or critical point identification in objects defining the digital topologies. The ridge identification brings back a huge set of ridge points which are pruned to obtain ridge point set of manageable dimensions in the second step. The discrete ridge points obtained from

the second step are connected based on varied algorithms like minimum spanning tree (H. Sundar *et al*, 2003), shortest path algorithm (L. Wade *et al*, 2002), LM path algorithms (I. Bitter *et al*, 2001) and a few more in the final step to obtain the skeleton curve. These algorithms are computationally less expensive when compared to the thinning and boundary based techniques and are highly efficient in the case of tubular digital topologies. On application to arbitrary digital topologies, the skeleton extraction achieved is inaccurate.

c. Geometric based Skeleton Extraction for Digital Topologies: In this technique the digital topology is represented in terms of scatter point sets or polygonal mesh structure. The Voronoi diagram is a common way to represent the digital topology (R. Ogniewicz *et al*, 1995) and the same is used to develop skeleton extraction in this work. To represent geometric 3D structures, a polyhedral technique is presented in Ref. (T. Culver *et al*, 2004). The geometric based techniques are computationally more intensive than the thinning and boundary based technique, and is applicable to medial surfaces.
d. Field Function Based Skeleton Extraction of Digital Topologies: In this technique, varied field functions are utilized to represent the fields and the functions are used to compute the skeleton curves. Radial Basis Functions (W. Ma *et al*, 2003), potential field functions (J. Chuang *et al*, 2000), electrostatic field function (T. Grigorishin *et al*, 1998), and visible repulsive force functions (F. Wu *et al*, 2005) are a few functions proposed by researchers. This skeleton extraction technique is robust even in the presence of noise in digital topologies and are computationally intense since several field equations need to be solved.

The above discussed skeleton extraction techniques cannot be applied to wireless sensor network topologies due to the discrete behavior that sensor networks exhibit. (J. Bruck *et al*, 2005) in their research work proposed a medial axis based naming and routing protocol. Therein, they have discussed about medial axis construction and routing protocols. The medial axis is constructed by identifying the skeleton nodes and the routing protocol exhibits efficient load distribution characteristics while routing connectivity based skeleton extraction algorithm for wireless sensor networks is discussed in Ref. (Hongbo Jiang *et al*, 2010). In that work, a coarse skeleton is constructed on the basis of boundary partitioning to identify the skeletal nodes, identifying the skeletal arcs and extending the connectivity amongst the skeletal arcs. The coarse skeleton is refined to finally extract the skeletal graph. The connectivity based skeleton extraction algorithm accurately preserves the network topology and extracts the skeleton of sensor network topologies even in the presence of noise. The use of the distance transform to extract skeletons from large scale wireless sensor networks is proposed in Ref. (Wenping Liu *et al*, 20013), wherein accurate or complete topology boundaries are not present. A node map is obtained by applying the distance transform and, using the distance map, the skeleton nodes are identified and connected using a controlled folding scheme to form a coarse skeleton. The shortest path trees are used to refine the coarse skeleton and obtain the skeleton of the sensor network topology. Network overhead reduction and robustness to noise is claimed in the research work presented in Ref. (Wenping Liu *et al*, 20013). In this paper, a skeleton extraction technique applicable to 3D wireless sensor network topologies is proposed and is presented in the next section.

3. Proposed System

3.1 Introduction

Let $\mathcal{T}$ represent a 3D wireless sensor network topology consisting of N sensor nodes and L links. The topology can be represented as a graph $\mathbb{G}\,(N\,,\,L)$. The Cartesian coordinates of the sensor node $n_a \in N$ can be represented as $p_{n_a} = \left(x_{n_a}\,,\, y_{n_a}\,,\, z_{n_a}\right)$. Let the set S represent the skeleton nodes or the critical nodes in the topology $\mathcal{T}$ that needs to be identified and set R represent the remaining nodes. The node set N can be defined as $N = S\,\cup R$.

Let r_t represent the transmission radius and the sensing radius be represented as r_s of a sensor node. The surface coverage of the N sensor nodes are complex spaces (Linghe Kong *et al*, 2013) and are defined as:

$$1-\left(1-\sum_i\left(\frac{(\mathcal{A}_i/\mathcal{A}_T)(2\pi^2r^2/2\pi(\pi r^2+\mathcal{A}_i)+2\pi r\mathcal{A}_i)}{((\mathcal{A}_i+\mathcal{P}_i r+\pi r^2)\cos\theta_i/(\mathcal{A}'_T+\mathcal{P}_T r+\pi r^2))}\right)\right)^{\lambda(\mathcal{A}'_T+\mathcal{P}_T r+\pi r^2)} \tag{1}$$

where $\mathcal{P}_\mathcal{T}$ is the perimeter,
λ is the sensor deployment intensity,
θ_i is the angle between $\mathcal{A}_i$ and xy plane and
$\mathcal{A}'_\mathcal{T}$ is the area of the z plane projection of $\mathcal{A}_i$.

The skeleton of the 3D wireless topology $\mathcal{T}$ is represented as a graph $\mathbb{G}_S(S\,,\,L_S)$, where L_S represents the skeletal links. As the skeleton is a part of the wireless sensor network topology graph, it can be stated that $\mathbb{G}_S \subset \mathbb{G}$. Let us consider the existing skeleton node represented as S_C that is common to all the skeletal links L_S and is the root node of the skeleton graph $\mathbb{G}_S$. The set L_S represents the skeletal links between the skeleton node S_C and a set of extreme sensor nodes represented by S_E. To construct the skeleton graph, we need to identify the skeletal links L_S, the skeleton nodes S and the root node S_C. The loss of topological information should be eliminated in the construction of the skeleton graph so that the skeleton extracted represents the topology $\mathcal{T}$ attributes accurately. A transmission based scheme is adopted to extract the skeleton similar to the method proposed in Ref. (Hassouna, M.S. *et al*, 2005) and Ref. (Thomas Deschamps *et al*, 2001). Each sensor node, called a source node, initiates a transmission to all the other sensor nodes in the topology, monitoring the energy utilized and the route response messages. This transmission mechanism is recursively repeated till all the sensor nodes are made as the source node. Based on the energy utilized, the skeletal links L_S are identified. Backtracking enables redundant link elimination and skeleton node S extraction. The root node S_C is identified and the skeleton $\mathbb{G}_S$ graph is constructed. The energy utilized during the transmission is determined heuristically in Ref. (Hassouna, M.S. *et al*, 2005, Thomas Deschamps *et al*, 2001) which is not applicable in the case of wireless sensor networks. To overcome this problem, the research work proposed here introduces a novel energy utilization function $\mathfrak{e}(n)$ to account for the energy utilized during transmission and to identify the skeletal links L_S.

3.2 Introduction of the Energy Utilization Function $\mathfrak{e}(n)$

Let the frequency based weight assignment function of a node $n \in N$ be represented as $\mathfrak{f}(n)$. The frequency based weight assignment is formulated in such a way that it assigns higher weight values to skeleton nodes $s \in S$ in comparison to the regular node $r \in R$, i.e., $\mathfrak{f}(s) > f(r)$.

A transmission based scheme is adopted to extract the skeleton graph $\mathbb{G}_S$. A sensor node in the sensor network $n_{src} \in N$ is considered as the source and all the remaining nodes are considered as the destination nodes and transmission is carried out. The assignment of the source node is recursively carried out until each sensor node $n \in N$ is considered as the source node n_{src}, i.e., $\forall\, n \in N : n_{src} = n$. Let us consider a transmission from the source node n_{src} at a location $p_{n_{src}} \in \mathcal{A}_{\mathcal{T}}$ to the sensor node n_{dst} located at $p_{n_{dst}} \in \mathcal{A}_{\mathcal{T}}$. The energy utilized in obtaining the optimal link route of the transmission is defined as

$$\mathcal{E}(n_{src}) = m \downarrow_{L_{n_{src}\,n_{dst}}} \int_{n_{src}}^{n_{dst}} \mathfrak{e}\left(L(n)\right) dn \tag{2}$$

where $L(n) : [0, \infty) \Longrightarrow L^n$ is the optimal energy route computation function,
$L_{n_{src}\,n_{dst}}$, is the routing table of the source sensor node n_{src} to the destination sensor node n_{dst} and
$m \downarrow_{L_{n_{src}\,n_{dst}}}$ represents the energy utilized for the minimum hop route from source node n_{src} to destination node n_{dst}.

Considering the physical radio layer transmission is $\mathcal{V}$, the energy utilized in obtaining the optimal route can also provide the least time interval for any active transmission from n_{src} to n_{dst}, i.e., $|\nabla \mathcal{E}(n_{dst})| \times \mathcal{V}(n_{dst}) = 1$. The energy utilized $\mathfrak{e}$ with respect to the radio layer transmission rate can be, therefore, defined as $\mathcal{V}(n_{dst}) = 1/\mathfrak{e}(n_{dst})$. The generalized form of the equation can be defined as

$$\mathcal{V}(n) = 1/\mathfrak{e}(n) \tag{3}$$

where $\mathcal{V}(n)$ is the radio layer speed function defined as $\mathcal{V}(n) = \chi\left(\mathfrak{f}(n)\right)$. In order to identify the skeletal links, let us consider a sensor node pair (n_i, n_j) and $l_{i,j}$ represents the link between them. For the link $l_{i,j} \in L_S$ and node $(n_i, n_j) \in S$, the energy utilized in the transmission between node n_i and node n_j is defined as

$$\mathfrak{e}(n) = e^{-\eta \mathfrak{f}(n)} \tag{4}$$

where $\eta > 0$ and is defined as

$$\eta > (1/\alpha) \ln\left(\sqrt{(d^2x + d^2y + d^2z)}/m \downarrow (dx, dy, dz)\right)$$

where dx, dy, dz is the spacing, $m\downarrow$ is the minimum function and α is the minimum value of the absolute difference between the neighboring sensor nodes.

Figure 3 gives the flowchart for finding the surface coverage using Equation 1. All the transmissions carried throughout the network are monitored and the energy utilized is observed if the transmission over a link satisfies the value computed by Equation 4 then it is identified as the skeletal link and the nodes on the link as the skeleton nodes. A detailed explanation is provided in the latter section of this paper.

3.3. Root Node Sc Identification

In order to model the transmission carried throughout the topology, the authors adopt the contour or snake model introduced in Ref. (Chenyang Xu *et al*, 1997) to obtain the skeleton nodes of the 3D wireless sensor network. The snake or vector used to represent the transmissions that propagate through $\mathcal{T}$ may be defined as follows:

$$V_S(n) = [u_S(n) v_S(n) w_S(n)]^A \tag{5}$$

where $n = (x, y, z)$ are the 3D coordinates.

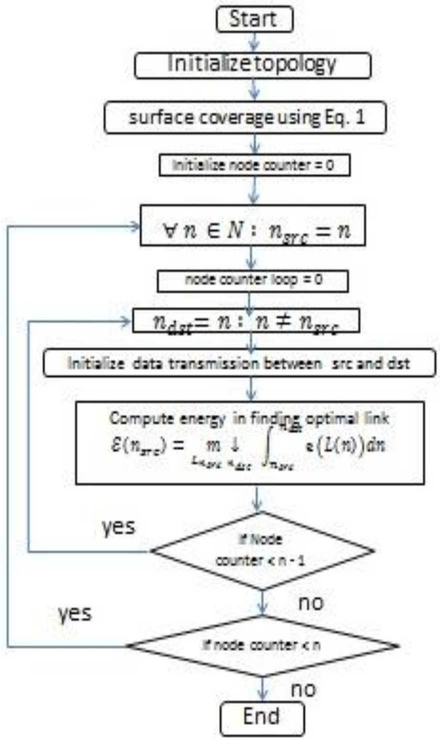

Fig. 3 Energy Utilization Function

Let $f_S(n)$ represent the edge map and μ represent the parameter of regularization, the snake $V_S(n)$ minimizes the energy function and can be defined as follows

$$\mathcal{E}_S(V_S) = \iiint \left(\mu\left(|\nabla u_S(n)|^2 + |\nabla v_S(n)|^2 + |\nabla w_S(n)|^2\right)\right) + \left(|f_S(n)|^2 |V_S(n) - \nabla f_S(n)|^2 dn\right) \tag{6}$$

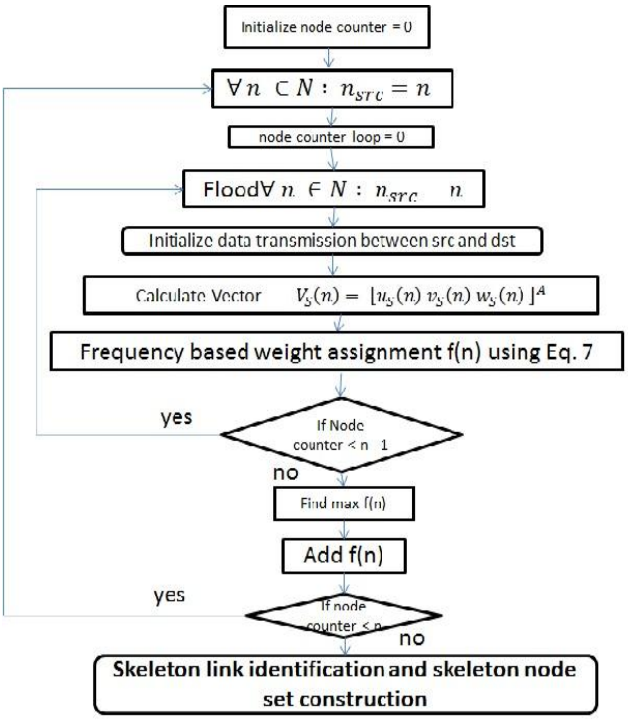

Fig. 4 Root Node Identification

The energy function $\mathcal{E}_S$ of the snake of the V_S is dominated by the partial derivatives of the primary term in the case where $\nabla f_S(n)$ is small. In the case where $\nabla f_S(n)$is large, $\mathcal{E}_S(V_S)$ is greatly dominated by the second term and the energy involved can be minimized by assuming $V_S = \nabla f_S(n)$. The use of generalized diffusion equations is considered to find the solution of the snake $V_S(n)$. The $V_S(n)$ of the n^{th} node is computed from the remaining node points in the topology $\mathcal{T}$ by utilizing a diffusion based procedure and these computations converge to a set of skeleton links $l \in L_S$. The diffusion based procedure is slow by nature and converges towards the center of the topology and in order to compute $\mathbb{G}_S$, we define the frequency based weight assignment $\mathfrak{f}(n)$ as follows where $m\uparrow$ is the max function and $m\downarrow$ is the min function.

$$\mathfrak{f}(n) = 1 - ((|V_S(n)| - m\downarrow|V_S|)/(m\uparrow|V_S| - m\downarrow|V_S|))^{\omega} \quad (7)$$

The parameter ω represents the strength and is assigned values between 0 and 1 . The parameter ω is assigned empirically. The weight assignment function defined above enables faster computations and convergence.

The S_C point is a skeleton node that belongs to all the links defined by $L_S$and can be obtained based on the frequency based weight assignment function $\mathfrak{f}(n)$. The sensor node with the maximum value of $\mathfrak{f}(n)$ is set to S_C. The computation of S_C is iteratively achieved and if another node whose weight is higher than S_C, then a new one is considered. The computation of S_C may be defined as:

$$S_C = \sum_{p=0}^{p=n} \left(m\uparrow\left(\mathfrak{f}(p)\right)\right) \quad (8)$$

Figure 4 presents the flowchart to identify S_C points as skeleton nodes that belong to links obtained based on frequency based weight assignment function using Equation 7. The skeleton link identification and skeleton node set construction is depicted in Figure 5.

3.4 Skeleton Links Ls Identification and Skeleton Node Set S Construction

The skeleton links L_S is a set of skeleton links l_s derived from the weight assignment function $\mathfrak{f}(n)$. To obtain L_S, the singular skeleton link l_s need to be obtained. Let us consider a skeleton node pair represented by (S_C, S_X). Let the sensor node $S_C$initiate a transmission signal to sensor node S_X. Let l_s represent the skeleton link that exists between the skeleton node pair (S_C, S_X). The skeleton link l_s corresponding to the minimum energy utilized between the nodes S_C and S_X and is based on equation (8). Let T be the time taken for the transmission from S_C to S_X. Tracking route reply from S_X to S_C would enable the identification of l_s and this process is defined as:

$$S_{n+1} = S_n - h(dT/|dT|)\,, S(0) = S_X \quad (9)$$

where h represents the error step. Using ordinary differential equations, the above equation can be represented as:

$$dl/dr = -(dT/|dT|)\,,\ S(0) = S_X \quad (10)$$

where r represents the route reply path from S_X to S_C. Adopting the Second order Range-Kutta theorem where the stages $\mathscr{k}_1 = f(S_n)$, $\mathscr{k}_2 = f(S_n + (h/2)\mathscr{k}_1)$ and $f(S_n) = -(dT(S_n)/|dT(S_n)|)$, the above equation can be represented as:

$$S_{n+1} = S_n + (h \times \mathscr{k}_2) \quad (11)$$

Having obtained a single skeleton link l_s, the process is iteratively repeated to obtain the entire skeleton links L_S for all the remaining sensor nodes $s \in S \mid s \neq S_C$. The iterative process exhibits multiple overlapping links which can be eliminated by tracking the route reply paths. The sensor nodes that exist on the skeleton links are the critical nodes or skeleton nodes and are represented by the set S.

3.5 $\mathbb{G}_S$ Skeleton Graph Construction

Having obtained the skeleton links L_S and the skeleton node set S, we shall now discuss the methodology adopted in constructing the skeleton graph $\mathbb{G}_S$. The skeleton graph is obtained by constructing layered topological sets. The layered topological sets are constructed by decomposing the sensor network topology $\mathcal{T}$ into topological clusters that represent the prominent 3D shape information of the topology. The skeleton sensor node S_C is considered as the root node of the skeleton graph $\mathbb{G}_S$. Each topological cluster consists of a set of regular sensor nodes and a skeleton node. In other terms, each skeleton node is used to represent a cluster and the skeleton links form the boundary of that cluster. The cluster is identified in terms of the relative distance from the skeleton node S_C. The skeleton graph $\mathbb{G}_S$ is constructed from the layered topological sets, wherein the skeleton nodes represent a cluster and the skeleton links represent the boundaries. On constructing the $\mathbb{G}_S$, it is observed that the leaf nodes of the graph can be used to identify the topological information of the sensor network $\mathcal{T}$.

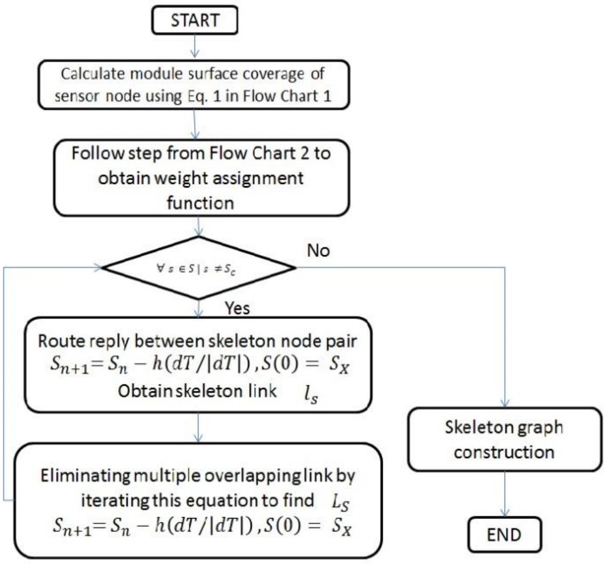

Fig. 5 Skeleton Link Identification

The construction of the layered topological clusters is critical to obtain the skeleton graph $\mathbb{G}_S$ without the loss of topological information. Let $Q(n)$ represent the distance function. A transmission with a speed parameter ρ $(\rho > 0)$ is propagated from the skeleton node S_C that can be represented as a partial differential equation. The solution of the partial differential equation results in a novel distance function represented as $Q'(n)$. The speed of the transmission is defined as $\mathcal{V}(n) = e^{-\rho Q(n)}$. To derive the function $Q(n)$, it is required to define parameter ρ .

Let us consider a skeleton link $l_S \in L_S$ that exists between two skeleton node pair (S_C, S_X). Let there be n regular sensor nodes having $(n-1)$ links that exist between the skeleton node pair (S_C, S_X). Let the skeleton transmit a packet from S_C to S_X with a speed represented as ρ. If t_{S_a} represents the time taken to transmit the packets amongst two adjacent sensor nodes, then the time taken to reach the destination may be defined as $T = \sum_{a=1}^{n-1} t_{S_a}$. The variable is obtained using $t_{S_a} = D(n_{a-1}, n_a)/\mathcal{V}(n_a)$. Let us consider time t' greater than t_{S_a}, i.e., $(t' > t_{S_a})$ and define t' as:

$$t' \leq D(n_{a-1}, n_a)/e^{\rho \mathfrak{f}(n_a)} \quad (12)$$

Rearranging the terms of equation (12), ρ can be represented as:

$$\rho \leq (1/\mathfrak{f}(n_a)) \times (\ln(D(n_{a-1}, n_a)/t')) \quad (13)$$

Considering $\mathfrak{f}(n_a) = \mathfrak{f}_{m\uparrow}$ and $D(n_{a-1}, n_a) = m \downarrow (dx, dy, dz)$, the value of ρ would result in the worst case scenario. Let ρ' represent the critical value of ρ and may be defined as:

$$\rho' \leq (1/\mathfrak{f}_{m\uparrow}) \times (\ln(m \downarrow (dx, dy, dz)/t')) \quad (14)$$

where $0 < t' < m \downarrow (dx, dy, dz)$ and if $t' = m \downarrow (dx, dy, dz)$, then $\rho' = 0$, which means that the transmission around the S_C skeleton is uniform and, the layered topological clusters formed are not accurate. To avoid such scenarios, the authors consider $0 < t' < m \downarrow (dx, dy, dz)$.

The time discretized version of the function $Q'(n)$ is defined as:

$$\overline{Q'(n)} = [Q'(n)] \quad (15)$$

Rapid discretization is not considered as $[Q'(n)]$ would not result in non-accurate layered topological cluster formulations. All the skeleton nodes having the same $\overline{Q'(n)}$ form a cluster, provided they are not adjacent to one another. In $\mathbb{G}_S$ the root node is the topological cluster containing the skeleton node S_C followed by the clusters exhibiting increasing values of $\overline{Q'(n)}$. Two skeleton nodes in the $\mathbb{G}_S$ are said to be connected if there is a skeleton link between them. The two topological clusters are said to be adjacent if the ancestor skeleton node is common and there exists a skeleton link amongst them.

The identification of the critical sensor nodes or skeleton nodes in the 3D topology $\mathcal{T}$ is represented as a skeleton graph $\mathbb{G}_S(S, L_S)$ consisting of skeleton nodes and skeletal links. The experimental study of the proposed skeleton extraction on varied 3D topologies is discussed in the subsequent section of the paper.

4. Implementation of Skeleton Extraction Algorithm

In order to evaluate the skeleton extraction algorithm, the authors of this paper have considered 3D topologies obtained from the AIM@SHAPE Shape Repository (AIM@SHAPE shape repository). The sensor nodes are deployed on the varied topologies to achieve complete coverage. The routing algorithm is adopted from Ref. (Zussman. G *et al*, 2003) and, the energy efficient TDMA MAC from Ref. (Rong gang Bai *et al*, 2007) is considered for communication amongst the sensor nodes. The entire proposed skeleton extraction algorithm presented earlier has been implemented using **C#** in custom simulation environment and performance evaluated. Two scenarios were considered for evaluation for each of the topologies. In the first scenario, a uniform sensor node configuration is considered and is referred to as the balanced scheme. In the second scenario, the skeleton extraction is performed and additional battery resources are provided to the skeleton nodes and referred to as the Additional Resource System. Uniform sensing events are induced in both the scenarios throughout the network. The network drop rate and the average sensor node energy remaining with respect to the simulation time are monitored. The authors have considered the Chianti hills terrain (AIM@SHAPE DIGITAL SHAPE WORKBENCH 5.0."Model name: Chianti hills , ID: 792 "), Crater terrain (AIM@SHAPE DIGITAL SHAPE WORKBENCH 5.0."Model Name: Crater, ID:71") and the Dolomites Mountain terrain (AIM@SHAPE DIGITAL SHAPE WORKBENCH 5.0."Model name: Dolomites, ID: 869") for the Sensor Network performance evaluation.

4.1 Evaluation Considering Chianti hills terrain

The Chianti Hill Terrain considered is shown in Figure 6. A total of 130 sensor nodes are deployed over the terrain area. The skeleton and the skeleton nodes extracted are shown in Figure 7. For the balanced system and the Additional Resource System, the network drop rate obtained is presented in Figure 8. The results obtained prove that the proposed AR system exhibits a lower network drop rate when compared to the proposed balanced system. Provisioning of additional resources to the critical or skeleton nodes mainly contributes to the ***reduction in the network drop rate*** by about ***29%***.

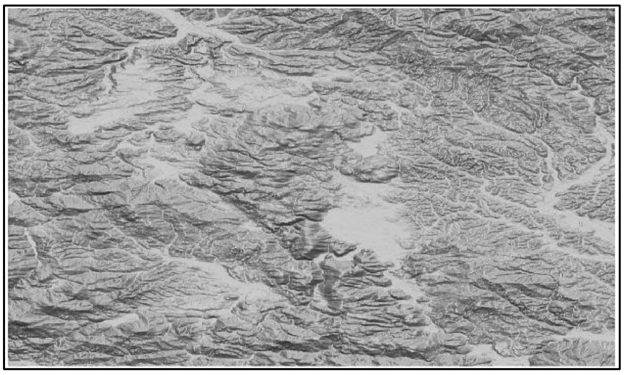

Fig. 6 Chianti Hill Terrain

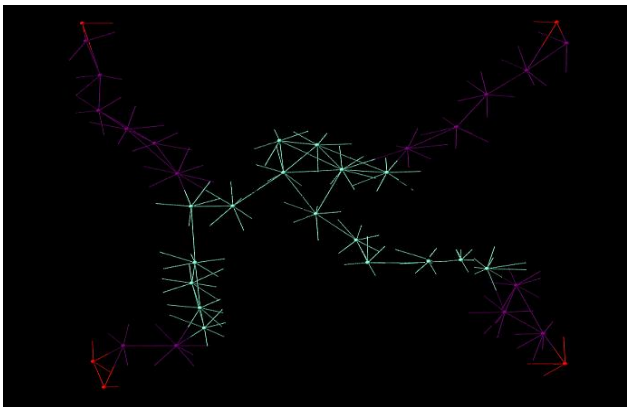

Fig. 7 Skeleton and Skeleton Nodes for Chianti Hill Terrain

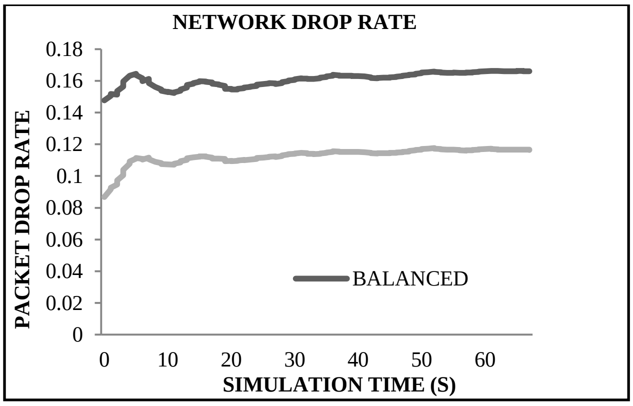

Fig. 8 Network Drop Rate Versus Time for Chianti Hill Terrain

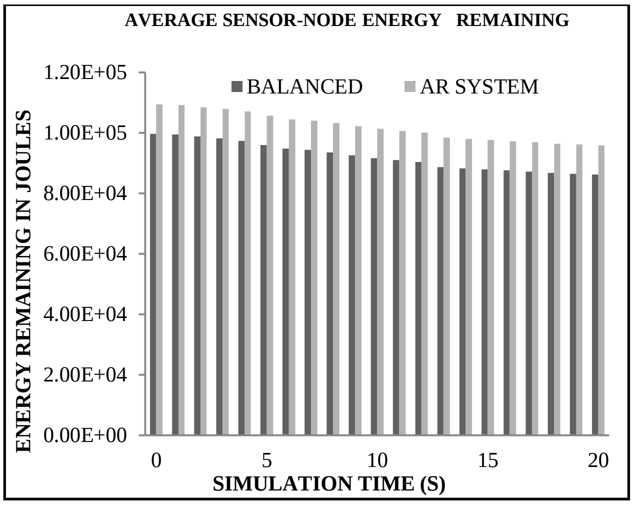

Fig. 9 Average Sensor Node Energy Conserved Vs Simulation Time Obtained for Chianti Hill Terrain

In addition to the network drop rates, the average remaining sensor node energy is also plotted and is presented in Figure 9. From the graph it is clear that the ***additional resources allocated to the skeleton nodes are beneficial in increasing the network life time*** which is dependent on the average sensor network energy remaining.

4.2 *Evaluation Considering Crater Terrain*

The terrain represents the 3D topology of a half crater and is shown in Figure 10 of this paper. Complete coverage of this terrain was achieved by deploying 261 sensor nodes with 6966 wireless links. The consideration of this model proves that the skeleton extraction algorithm is applicable to cases where the depth of the terrain is very large. The skeleton extraction results obtained is shown in Figure 11. From the figure, it is observed that the skeleton extracted consists of 72 skeleton nodes. The sensor network deployed is simulated using the proposed Balanced and Additional Resource System inducing uniform sensing events.

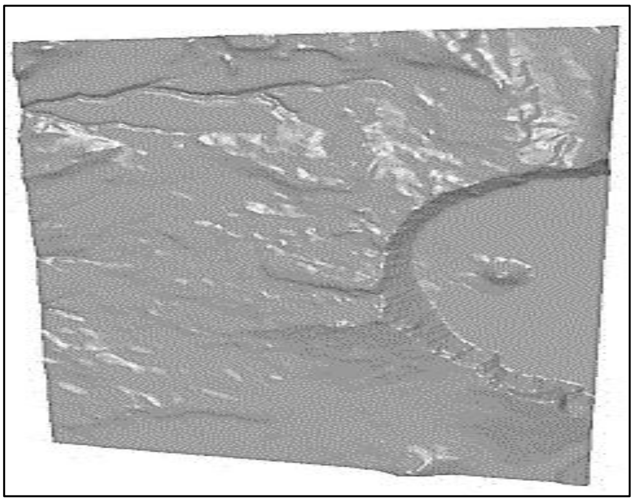

Fig. 10 Crater Terrain

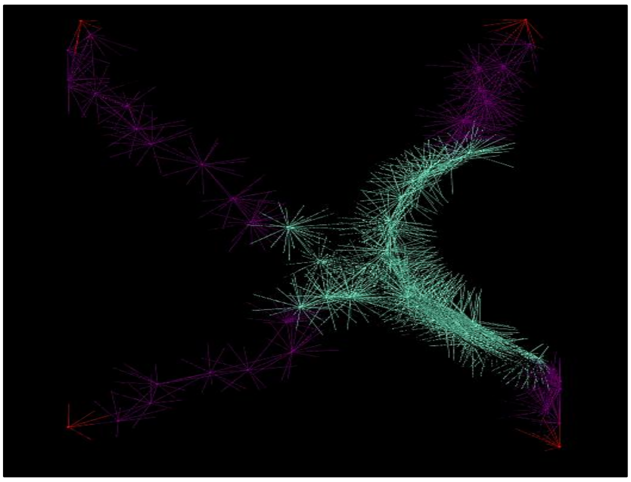

Fig. 11 Skeleton and Skeleton Nodes for Crater Terrain

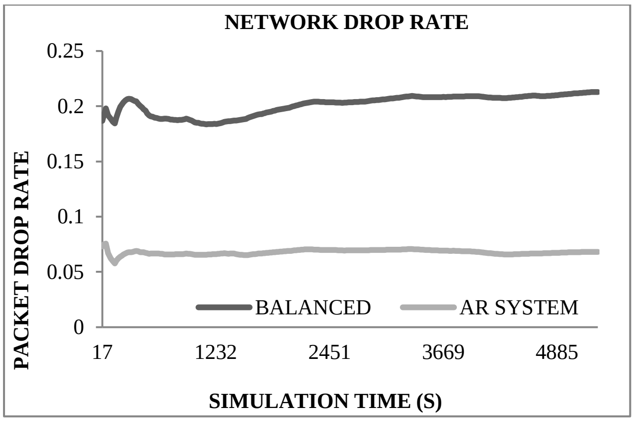

Fig. 12 Network Drop Rates Observed for Crater Terrain

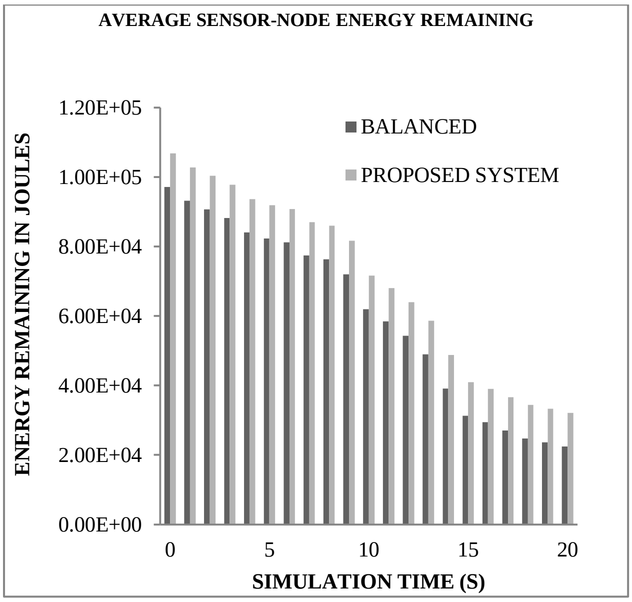

Fig. 13 Average Sensor Node Energy Conserved Vs Simulation Time Observed for Crater Terrain

The network packet drop rates and the average sensor node energy remaining results obtained from the simulation are presented in Figure 12 and Figure 13 respectively. From these results, it can be concluded that the proposed scheme reduces the network drop rate by 66.3% and the average sensor node energy conserved is 13.8%.

4.3 Evaluation Considering Dolomites Mountain Terrain

The famous Dolomites mountain terrain of Italy considered is shown in Figure 14.

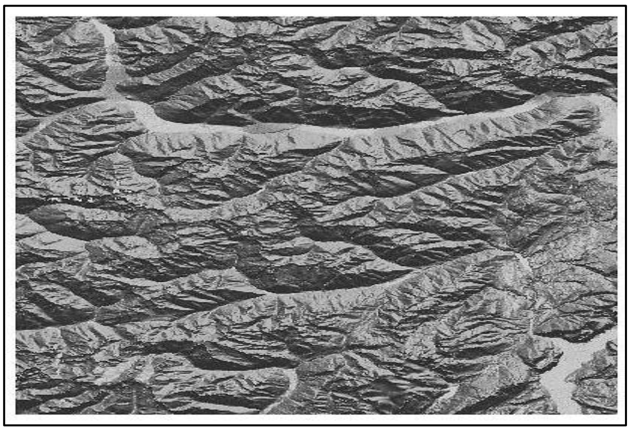

Fig. 14 Dolomities Mountain Terrain

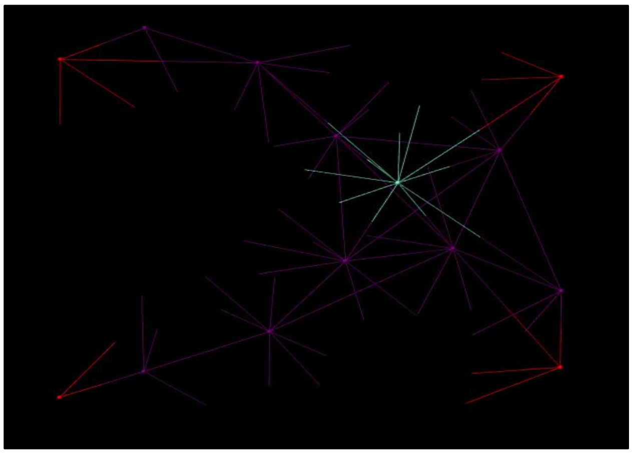

Fig.15 Skeleton and Skeleton Nodes for Dolomites Mountain Terrain

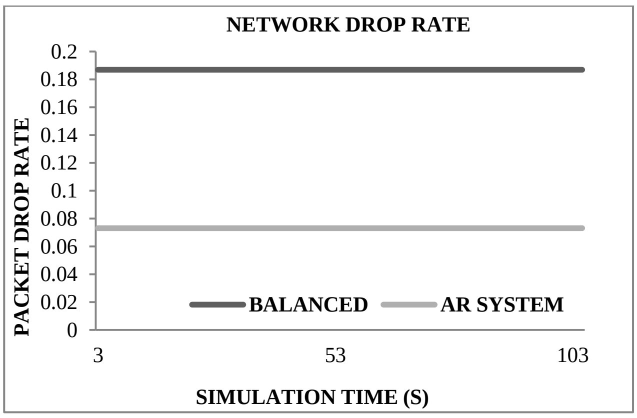

Fig.16 Network Drop Rates Observed for Dolomities Mountain Terrain

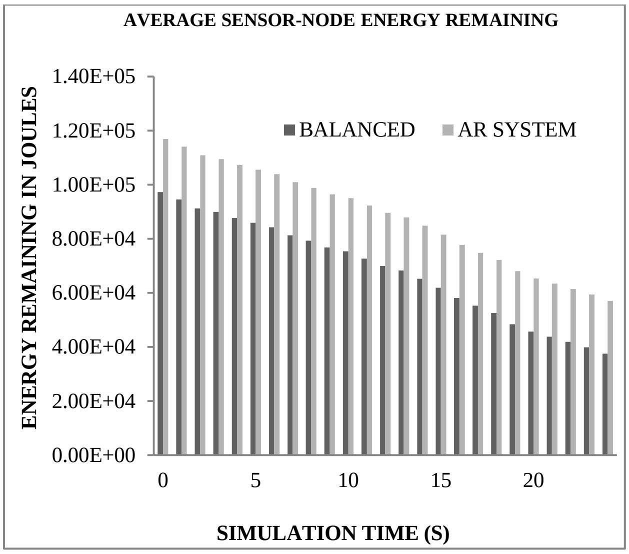

Fig.17 Average Sensor Node Energy Conserved Vs Simulation Time Observed for Dolomites Mountain Terrain.

A total of 25 sensor nodes are considered to be deployed in this terrain to achieve complete coverage. The extensive terrain variation in the Dolomites Mountains is an issue, hence this terrain is considered in the evaluation of the skeleton extraction algorithm. The skeleton extracted of 14 sensor nodes is shown in Figure 15. The sensor network is simulated using the balanced and Additional Resource System scheme by inducing uniform sensing events throughout the network. The results obtained are shown in Figure 16 and 17. The packet drop rate is reduced by about 60% and the average sensor node energy conserved is about 22.3% when compared to the proposed balanced scheme.

Conclusions

Sensor Networks are widely adopted for varied applications in the real world scenario. Accurate data aggregation and minimum energy utilization are desired features to be achieved from sensor network deployments. Provisioning of additional resources to certain sensor nodes has proved to improve sensor network performance. In this paper, in order to identify the nodes to which additional resources have to be provided, a skeleton extraction algorithm has been developed and implemented using C#. The skeleton extraction algorithm proposed considers the complex 3D coverage model of sensor nodes to render it realistic and applicable. The energy utilization function discussed in this paper is used to identify the skeleton link and nodes. The skeleton extracted is represented as a graph and its root node is identified by the weight assignment function. The 3D topological information is preserved by adopting a clustering technique in the proposed skeleton extraction algorithm. Varied complex 3D terrains have been considered. The simulation results presented prove that providing additional energy resources to the skeleton nodes improve network data aggregation owing to the reduction of network drop rate. The simulation results also prove that the average energy conserved improves by providing additional resources to the skeleton nodes. From the experimental study, it is observed that the network performance is enhanced and energy conservation achieved is about 20 %.

References

Robert Szewczyk, Eric Osterweil, Joseph Polastre, Michael Hamilton, Alan Mainwaring, and Deborah Estrin (2004), Habitat monitoring with sensor Networks, *Commun. ACM 47*, pp 34-40. DOI: 10.1145/990680.990704. http:// doi.acm.org/10.1145/990680.990704.

Kumar. P, Young-Dong Lee, Young-Dong Lee (2010), "Secure health monitoring using medical wireless sensor networks," *Networked Computing and Advanced Information Management (NCM),* 2010 Sixth International Conference on , pp. 491-494.

M. Fennell and R. Wishner (1998), Battlefield Awareness via Synergistic SAR and MTI Exploitation, *IEEE Aerospace and Electronic Systems Magazine*, Vol. 13, No. 2, pp. 39-43.

M. Younis and K. Akkaya (2008), Strategies and techniques for node placement in wireless sensor networks: a survey, *Ad Hoc Networks*, Vol. 6, No. 4, pp. 621–655.

Yonghyun Kim, Myungho Yeo, Daesik Kim, and Kwangsue Chung (2012), A Node Deployment Strategy Considering Environmental Factors and the Number of Nodes in Surveillance and Reconnaissance Sensor Networks, *International Journal of Distributed Sensor Networks,* Vol. 2012, Article ID 385282. DOI:10.1155/2012/385282.

Zhao Cheng, Perillo M., Heinzelman W. B. (2008), General Network Lifetime and Cost Models for Evaluating Sensor Network Deployment Strategies, *Mobile Computing, IEEE Transactions on* ,Vol. 7, No. 4, pp. 484-497

X. Bai, D. Xuan, Z. Yun, T. H. Lai, and W. Jia (2008), Complete optimal deployment patterns for full-coverage and k-connectivity (k≤6) wireless sensor networks", *ACM MobiHoc,* Pages 401– 410, New York, NY, USA.

S. Kumar, T. H. Lai, and A. Arora (2005), Barrier coverage with wireless sensors, *ACM MobiCom*, pp 284–298, New York, NY, USA.

C. F. Huang, Y. C.Tseng, and L. C. Lo (2004), The coverage problem in three-dimensional wireless sensor networks, *IEEE GLOBECOM*, Vol. 5, pp 3182–3186

M. Watfa and S. Commuri (2006). A coverage algorithm in 3D wireless sensor networks. *IEEE PerCom*.

Linghe Kong, Mingchen Zhao, Xiao-Yang Liu, Jialiang Lu (2013), Surface Coverage in Sensor Networks, *IEEE Transactions on Parallel and Distributed Systems,* 25, *IEEE computer Society Digital Library,* IEEE Computer Society,http://doi.ieeecomputersociety.org/10.1109/TPDS.2013.35

http://fiji.eecs.harvard.edu/Volcano/.

S. K. Pushpa, S. Ramachandran and K. R. Kashwan (2013), A Novel Skeleton Extraction Algorithm for 3D wireless Sensor Networks, *Global Journal of Computers Science and Technology,* Vol. 13, No. 16-E, pp. 30-45.

N. D. Cornea, D. Silver, and P. Min (2005), Curve-Skeleton Applications," *Proc. IEEE Visualization Conf. (VIS '05)*

J. W. Brandt and V. R. Algazi (1992), Continuous Skeleton Computation by Voronoi Diagram, *CVGIP: Image Understanding,* Vol. 55, No. 3, pp. 329-338, 1992

N. Gagvani and D. Silver (2001), Animating Volumetric Models, *Graphical Models,* Vol. 63, No. 6, pp. 443-458.

S. R. Aylward and E. Bullitt (2002), Initialization, Noise, Singularities and Scale in Height Ridge Traversal for Tubular Object Centerline Extraction, *IEEE Trans. Medical Imaging*, Vol. 21, No. 2, pp. 61-75.

J. Bruck, J. Gao, and A. A. Jiang (2005), MAP: Medial Axis Based Geometric Routing in Sensor Networks, *Proc. ACM MobiCom*.

Hongbo Jiang, Wenping Liu, Dan Wang, Chen Tian, Xiang Bai, Xue Liu, Ying Wu, Wenyu Liu (2010), Connectivity-Based Skeleton Extraction in Wireless Sensor Networks, *Parallel and Distributed Systems, IEEE Transactions on* , Vol.21, No.5, pp.710-721, DOI: 10.1109/TPDS.2009.109

Wenping Liu, Hongbo Jiang, Xiang Bai, Guang Tan, Chonggang Wang, Wenyu Liu, KechaoCai (2013), Distance Transform-Based Skeleton Extraction and Its Applications in Sensor Networks, *Parallel and Distributed Systems, IEEE Transactions* on , Vol. 24, No. 9, pp. 1763-1772, DOI: 10.1109/TPDS.2012.300.

Cornea, N. D., Silver, D., Min. P. (2007), Curve-Skeleton Properties, Applications, and Algorithms, *Visualization and Computer Graphics, IEEE Transactions* on ,Vol. 13, No.3, pp.530-548, DOI: 10.1109/TVCG.2007.1002.

D.G. Morgenthaler (1981), Three-Dimensional Simple Points: Serial Erosion, Parallel Thinning and Skeletonization, TR-1005, *Computer Vision Lab*., Univ. of Maryland.

H. Sundar, D. Silver, N. Gagvani, and S. Dickinson (2003), Skeleton Based Shape Matching and Retrieval, *Proc. Shape Modeling Int'l Conf.*, 2003.

L. Wade and R.E. Parent (2002), Automated Generation of Control Skeletons for Use in Animation, *The Visual Computer*,Vol. 18, No. 2, pp. 97-110.

I. Bitter, A.E. Kaufman, and M. Sato (2001), Penalized-Distance Volumetric Skeleton Algorithm, *IEEE Trans. Visualization and Computer Graphics*,Vol. 7, No. 3.

R. Ogniewicz and O. Ku¨ bler (1995), Hierarchic Voronoi Skeletons, *Pattern Recognition*, Vol. 28, No. 3.

T. Culver, J. Keyser, and D. Manocha (2004), Exact Computation of the Medial Axis of a Polyhedron, *Computer Aided Geometric Design*, Vol. 21, No. 1, pp. 65-98.

W. Ma, F. Wu, and M. Ouhyoung (2003), Skeleton Extraction of 3D Objects with Radial Basis Functions, *Proc. IEEE Int'l Conf. Shape Modeling and Applications*.

J. Chuang, C. Tsai, and M.-C. Ko (2000), Skeletonization of Three- Dimensional Object Using Generalized Potential Field, *IEEE Trans. Pattern Analysis and Machine Intelligence*, Vol. 22, No. 11, pp. 12-41.

T. Grigorishin and Y.H. Yang (1998), Skeletonization: An Electrostatic Field-Based Approach, *Pattern Analysis and Applications*, Vol. 1, pp. 163-177.

F. Wu, W.C. Ma, P. Liou, R. Liang, and M. Ouhyoung (2005), Skeleton Extraction of 3D Objects with Visible Repulsive Force, *Proc. EurographicsSymp. Geometry Processing.*

Hassouna M. S., Farag A. A. (2005), Robust centerline extraction framework using level sets, *Computer Vision and Pattern Recognition,* CVPR 2005. IEEE Computer Society Conference, Vol.1, pp. 458-465, 20-25, DOI: 10.1109/CVPR.2005.306.

Thomas Deschamps, Laurent D. Cohen (2001), Fast extraction of minimal paths in 3D images and applications to virtual endoscopy, *Medical image analysis* 1 December 2001, Vol. 5, No. 4, pp. 281-299, DOI: 10.1016/S1361-8415(01)00046-9.

Chenyang Xu, Princ, J. L. (1997), Gradient vector flow: a new external force for snakes, *Computer Vision and Pattern Recognition. Proceedings, IEEE Computer Society Conference,* pp. 66-71, DOI: 10.1109/CVPR.1997.609299.

Aim@Shape shape repository. http://visionair.ge.imati.cnr.it/

Zussman G., Segall A. (2003), Energy efficient routing in ad hoc disaster recovery networks, INFOCOM. *Twenty-Second Annual Joint Conference of the IEEE Computer and Communications, IEEE Societies*, Vol. 1, No., pp. 682-691, DOI: 10.1109/INFCOM.2003.1208718.

Rong gang Bai, Yu-gui Qu, Yang Guo, Bao-hua Zhao (2007), An Energy-Efficient TDMA MAC for Wireless Sensor Networks, *Asia-Pacific Service Computing Conference, The 2nd IEEE* , pp. 69-74, DOI: 10.1109/APSCC.2007.25.

Aim@Shape Digital Shape Workbench 5.0."Model name: Chianti hills , ID: 792 ", Website: http://visionair.ge. imati.cnr.it: 8080/ontologies/ shapes/view.jsp?id=792-Chianti_ hills.

Aim@Shape Digital Shape Workbench 5.0."Model Name: Crater, ID:71", URL: http:// visionair.ge .imati.cnr.it:8080/ ontologies/ shapes/view.jsp? id=71-Crater.

Aim@Shape Digital Shape Workbench 5.0."Model name: Dolomites, ID: 869", http://visionair.ge.imati.cnr.it:8080/ ontologies/shapes/view.jsp?id=869-Dolomites.